SCIENCE CHINA Materials REVIEW

mater.scichina.com link.springer.com

Published online 18 September 2018 | https://doi.org/10.1007/s40843-018-9336-1

Sci China Mater 2019, 62(2): 161–172

Elucidating the dynamics of solvent engineering for perovskite solar cells

Zulqarnain Arain[1,3], Cheng Liu[1], Yi Yang[1], M. Mateen[1], Yinke Ren[1], Yong Ding[1*], Xuepeng Liu[1], Zulfiqar Ali[2], Manoj Kumar[3] and Songyuan Dai[1*]

ABSTRACT Researchers working in the field of photovoltaic are exploring novel materials for the efficient solar energy conversion. The prime objective of the discovery of every novel photovoltaic material is to achieve more energy yield with easy fabrication process and less production cost features. Perovskite solar cells (PSCs) delivering the highest efficiency in the passing years with different stoichiometry and fabrication modification have made this technology a potent candidate for future energy conversion materials. Till now, many studies have shown that the quality of active layer morphology, to a great extent, determines the performance of PSCs. The current and potential techniques of solvent engineering for good active layer morphology are mainly debated using primary solvent, co-solvent (Lewis acid-base adduct approach) and solvent additives. In this review, the dynamics of numerously reported solvents on the morphological characteristics of PSCs active layer are discussed in detail. The intention is to get a clear understanding of solvent engineering induced modifications on active layer morphology in PSC devices *via* different crystallization routes. At last, an attempt is made to draw a framework based on different solvent coordination properties to make it easy for screening the potent solvent contender for desired PSCs precursor for a better and feasible device.

Keywords: perovskite, solvent engineering, Lewis acid-base, additive, coordination property

INTRODUCTION

For the last few years, photovoltaic technology has developed into a vibrant scientific field for study and knowledge. The advancement of novel materials has unlocked perspectives for the fabrication of economic and competent devices [1]. Perovskite materials ($MAPbX_3$, MA=methylammonium and X=I, Br, Cl) have been considered as the exciting and promising ingredients in fabricating photovoltaic cells owing to its excellent absorption efficiency, ambipolar semiconductor, and long diffusion length [2–4]. The power conversion efficiency (PCE) of the perovskite solar cells (PSCs) swiftly increases from 3.8% to 23.3% [5,6], approaching the photovoltaic performances of crystalline silicon thin film and GaAs [7]. Such swift improvement is unprecedented in the solar energy, and thus PSCs are considered as the most competitive contenders for the next generation photovoltaics [2,8,9].

With the progress of fabrication techniques, such as vacuum evaporation [10], sequential deposition technique [11], solvent engineering approach [12], vapour-assisted [13] and additive-assisted deposition [14], high-quality layers of perovskite with smooth surfaces and uniformity have been produced by handling its fast nucleation behaviour, where PbI_2 was usually employed as B and X site species with MAI on A site in the perovskite structure.

The active layer is a vital part of a high-performance PSCs. Generally, the solution processed perovskite film's surface morphology can be controlled by the crystallization rate and nucleation, in detail, controlling fast nucleation and delaying crystal evolution [15]. The diffusion length for charge carrier of $MAPbI_3$ was changed from hundreds of nanometers to hundreds of micrometers, subject to trap density [2,8,9,16–18]. Trap density resulting from grain boundaries and defects was reported to impede the diffusion of free charge carrier, causing non-radiative recombination and thus rigorously dropping the charge carrier lifetime and photoluminescence yield [19,20]. Millimetre range free-standing sole crystals

[1] Key Laboratory of Novel Thin-Film Solar Cells, North China Electric Power University, Beijing 102206, China
[2] Renewable Energy School, North China Electric Power University, Beijing 102206, China
[3] Energy system Engineering Dept. Sukkur IBA University, Sukkur, Pakistan
* Corresponding authors (emails: sydai@ncepu.edu.cn (Dai S); dingy@ncepu.edu.cn (Ding Y))

of perovskite evolved in precursor solution are likely to enhance significant charge carrier lifetime with least radiative recombination [8,9]; Yet, this might be difficult to implement on existing devices. However, the fabrication of PSCs with excellent reproducibility and high PCE still depends on the selection of suitable solvents or system of solvents. Out of numerous factors affecting the performance of the perovskite layer, the choice of solvent is important [21]. Herein, we discuss in detail the influence of reported solvent process on the PSC performance, such as primary solvent, co-solvent (Lewis-base adduct approach) and solvent additives.

PRIMARY SOLVENT

By now, for solution-processed perovskite photovoltaic cells *via* one-step or two-step deposition technique, polar aprotic solvents, like dimethylsulfoxide (DMSO) and dimethylformamide (DMF) were widely used to solubilize the precursors owing to their coordination ability to form stable intermediate phases such as PbI_2-DMSO or MAI-PbI_2-DMSO [22,23]. Along with these DMSO and DMF, *N*-methyl-2-pyrrolidone (NMP) and *γ*-butyrolactone (GBL) are also some of the commonly used aprotic solvents in the precursor solution [15,24–26]. All the reported solvents hold a robust electronegative polar group with C=O or S=O that make them able to coordinate with PbI_2 possibly [27–29].

The choice of solvent for the precursor solution is a key factor affecting the device morphology. The main criterion is that the desired solvent should be polar aprotic, which can dissolve the perovskite precursors. The physical properties, like vapor pressure and boiling point, should be noted during the desired crystallization route, that is, slow or fast. Lin *et al.* [30] found that the crystal nucleus of the $MAPbI_3$ film is the largest in two-step deposition method, as root-mean-square (RMS) value is the greatest when DMF (24.549 nm) was the solvent as compared to DMSO (21.316 nm), GBL (11.962 nm) and NMP (4.667 nm). The vapor pressure of DMSO, DMF, GBL, and NMP at room condition are 2.7, 1.5, 0.375 and 0.3 mmHg, respectively. Higher saturated vapor pressure can cause a lower boiling temperature and higher volatility which lead to fast crystallization, while higher boiling temperature can raise the temperature and time of crystallization.

The boiling temperature of DMF (153°C) is lower than the others, so the crystal nucleus is steadily reaching substantial in size. Though the vapor pressure of DMF is lower than DMSO, crystal nucleus of DMSO is smaller because the dimension of the crystal nucleus is dependent

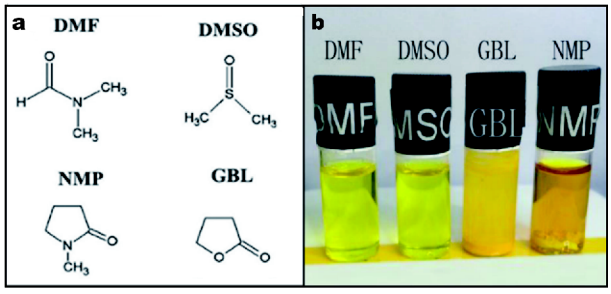

Figure 1 (a) Molecular arrangement of DMF, GBL, NMP, and DMSO. (b) The solubility of the PbI_2 precursor at 75°C in DMF, DMSO, GBL, and NMP. Both DMSO and DMF: liquefied; GBL: colloidal suspension; NMP: partially liquefied. Reprinted with permssion form Ref. [30], Copyright 2014, the Royal Society of Chemistry.

on not only solvent's volatility but also the strength of coordination with precursor and its respective crystallization route. As presented in Fig. 1b, through a continuing investigation at elevated temperature, the solubility of the precursor in DMF and DMSO is looking quite better than GBL and far superior to NMP. The layer thickness also has a significant impact on the efficiency of the device. When NMP solvent was used, the thickness of the $MAPbI_3$ layer is around 432.5 nm. While for GBL, DMSO and DMF, it is about 530.2, 621.3 and 1,169 nm. It indicates that a balanced trade-off between volatility and coordination strength of solvent can lead to optimum layer thickness [30].

Seo *et al.* [31] also supported the above results by using these solvents as a lone solvent and solvent system (co-solvent). They found that almost all of these solvents are capable of forming stable intermediate phase (IP) with MAI and PbI_2 with different coordination condition. As depicted in Fig. 2a, XRD spectra of the adduct show that all solvents except GBL contain diffraction peaks at low angles, which are eventually faded away due to the annealing process, indicating that they are transformed into $MAPbI_3$ [23,29] as shown in Fig. 2b. As witnessed in

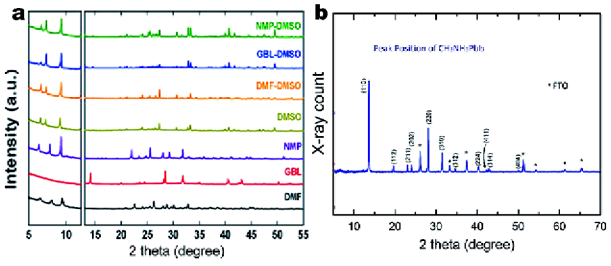

Figure 2 (a) X-ray diffraction (XRD) spectra of intermediate phases from different solvents. Reproduced from Ref. [31], Copyright 2017, Elsvier. (b) Final perovskite film with crystal plane. Reproduced from Ref. [23], Copyright 2015, American Chemical Society.

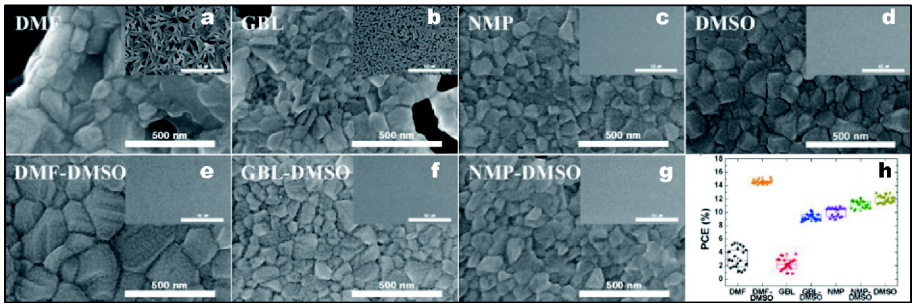

Figure 3 (a–g) Scanning electron microscopy (SEM) images of $MAPbI_3$ films processed using DMF, GBL, NMP, DMSO and their respective solvent system, respectively. Insets are at a scale bar of 10 μm. (h) PCE of the subsequent devices. Reproduced from Ref. [31], Copyright 2018, Elsvier.

previous studies, such low-angle IP peak demonstrates an intermediate state formation like MAI-PbI_2-DMF, MAI-PbI_2-NMP, and MAI-PbI_2-DMSO, and such observation on only low-angle IP peaks without $MAPbI_3$ peaks could also well support that the formed IP is relatively stable at room temperature, and it can slow down the perovskite nucleation [15,23,29,32]. The XRD pattern of the final $MAPbI_3$ film is shown in Fig. 2b. The sharp diffraction peaks centered at 14.2° (110 plane) and 28.5° (220 plane) along with other minor peaks are indicative of the $CH_3NH_3PbI_3$ phase, a crystal structure formed after annealing for a certain period.

Surface morphologies of subsequent layers (Fig. 3) display that the DMF and GBL processed films showed rough surfaces and poor uniformity with several holes and rod-shape grains. This poor uniformity could be due to the variance in solubility to endorse a different nucleation rate among both precursors and comparatively faster crystallization than in NMP and DMSO. On the other hand, NMP, DMSO, GBL-DMSO, and NMP-DMSO exhibited comparatively smooth morphology of perovskite films than DMF and GBL. DMSO exhibited significantly more uniform films among them, possibly due to the relatively slow crystallization rate than DMF and GBL. More remarkably, the DMF-DMSO formed better and matured films with grain size substantial than the lone DMSO, which might have been produced from the too slow removal of DMSO as a result of strong IP formation. Retarded crystallization always produces uniform film with smooth coverage, but grain size is not always substantial as compared to fast crystallization, causing more grain boundaries and subsequent recombination losses. In rapid crystallization of the perovskite solution, grain size grows up to substantial at the cost of film uniformity and coverage, resulting in trap states in the form of pinholes and non-aligned orientation of grains, which causes much more recombination losses than the former one. As shown in Fig. 3g, PCEs of the subsequent layers support the above-discussed facts. DMSO-based PSCs, particularly DMF-DMSO exhibited superior PCEs followed by NMP, owing to its smooth morphology with minimum trap states. While, lone DMF and GBL-based PSCs showed poor PCEs due to non-uniform coverage and voids, resulting in recombination losses.

Beside primary solvents assisted film passivation, a common tactic to improve the characteristics of perovskite film is to use a chloride-based precursor in the solution. In particular, $PbCl_2$ and CH_3NH_3I mixtures lead to the formation of larger crystal domains of the perovskite compared to other precursors and the related reduction of grain boundaries and defects in the film [33,34]. However, the role of chloride during the crystallization process is still unclear, with many studies reporting no or only small amounts of chloride in the final film as a result of gaseous byproduct that releases in the form of CH_3NH_3Cl during the annealing process. The difference in release and generation rate of CH_3NH_3Cl is of concern since it leads to the formation of pinholes and trap states resulting in substantial recombination rate and hysteresis in the final device. As previous studies, fast crystallization *via* hot casting and vacuum-assisted thermal annealing process can avoid this difference [33,35]. However, the problems with these processes are that either we need to maintain high temperature as in the case of hot casting (for both, solutions and subtract) or maintain vacuum for vacuum-assisted thermal annealing process, which are not scalable approaches regarding reproducibility. These non-scalable fast crystallization techniques can be replaced by such solvent engineering assisted fast nucleation method which does not require any stable IP formation.

Xiang *et al.* [36] developed a solvent-technique for even perovskite films without the need for high-temperature

annealing. NMP was used as a high-boiling-point solvent and a complexant, combined with the dimethylacetamide (DMAc, a homologous of DMF), to enhance the quality of perovskite films and improve the corresponding device performance. NMP has higher boiling temperature than DMSO, but if used in optimized volume ratio, its affinity towards strong non-polar anti-solvents can be a crucial advantage for rapid nucleation. Notably, 17.09% efficiency was attained even without any post-annealing process for the device based on DMAc/NMP co-solvents. The observed phenomenon is mainly because NMP-included solvents can induce an instant crystallization once the strong anti-solvent drips on the films at room temperature (RT). Although Xiang's work is based on standard CH_3NH_3I & PbI_2 precursors, still one can exploit the NMP's affinity towards non-polar anti-solvent for fast crystallization of chloride-based perovskite films without any post-annealing process. Since this solvent engineering technique does not need any annealing stage, so one can produce chloride based films without the generation of CH_3NH_3Cl which in other case is difficult to control.

From these annotations, it can be suggested that the balanced trade-off between solubility and physical properties (vapor pressure and boiling point) should be considered for selecting a primary solvent. The different IP formation can be the result of different solvents. Notably, since the IP degree could not be the same (MAI-PbI_2-DMSO>MAI-PbI_2-DMF>MAI-PbI_2-NMP>MAI-PbI_2-GBL) as known to be relative to the coordination strength amongst solvents (DMSO>DMF>NMP>GBL) and precursor [15,23,28,29,32,37–42]. These outcomes also indicate that each solvent can lead to different perovskite nucleation rate by either retarding or boosting the crystal evolution of precursor solution. This change in nucleation rate depends on the difference in IP stability and physical properties of solvents, like boiling point and vapor pressure as well as their behavior towards non-polar anti-solvent.

LEWIS ACID-BASE ADDUCT APPROACH

In most cases, the precursor solution for the one-step method involves more than one solvent as a co-solvent or solvent system. The intention is to form a stable Lewis acid-base adduct, leading to a homogeneous coverage and pinhole free morphology. Generally, it involves the use of one high boiling strong base polar aprotic solvent which can form a stable IP with precursor after quenching of low boiling solvent (volatile) due to anti-solvent washing, as illustrated in Fig. 4 [43,44]. Just like mentioned earlier, co-solvents are used to enhance the morphology of the perovskite layers [24]. Such solvent system produces crystals with appropriate grain dimensions to offer a better interfacial contact between the substrate and the active layer.

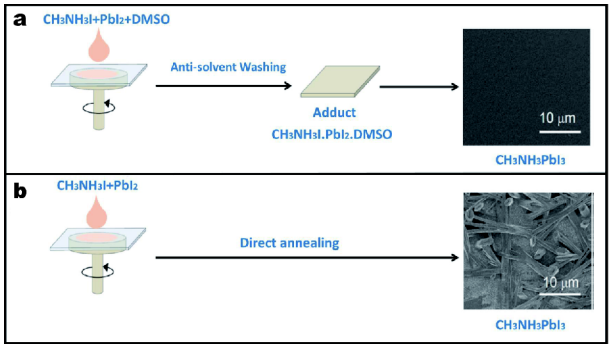

Figure 4 The depiction of the fabrication method and SEM images for perovskite films developed by deposition of the DMF solution (a) with DMSO and (b) without DMSO. To produce 1:1:1 adduct of MAI-PbI_2-DMSO, ethyl ether was loaded during a spin to quench out DMF. Reproduced from Ref. [23], Copyright 2015, American Chemical Society.

The reaction of an aprotic solvent (Lewis base) with Pb (II) halide (Lewis acid) results in the formation of the adduct, where adduct is coupled by a coordinate covalent bond (electrons shared by Lewis base) to make some coordination complex as typically happens in metal-ligand interactions in most organometallic compounds. The Pb(II) halides are recognized as Lewis acid since they receive iodide anion to make iodoplumbate anion like $[Pb_3I_{10}]^{4-}$ and $[Pb_5I_{16}]^{6-}$ [45,46]. It was stated that Pb(II) halides can form 1:1, 1:2, or 2:1 adducts with bidentate (LL) and monodentate (L) ligands with nitrogen, sulfur and oxygen donors [47,48], like DMSO, NMP, thiourea, thioacetamide, aniline, and pyridine. Ahn *et al.* [23] elucidated the Lewis acid-base adduct method for perovskite film evolution by using DMF and DMSO in precursor solution and found that stretching vibration of S=O ($\nu_{S=O}$) lies at 1,045 cm^{-1} for the pristine DMSO [49], which is moved to lower 1,020 cm^{-1} for PbI_2-DMSO complex and for MAI-PbI_2-DMSO complex it further moved down to 1,015 cm^{-1} (Fig. 5 and Table 1). The $\nu_{S=O}$ at 1,020 cm^{-1} is relatively steady with the frequency of 1,022 cm^{-1} noticed for the 1:1 adduct of PbI_2-DMSO [47].

Harmonic motion for diatomic model states that vibration frequency is relative to force constant's square root [50]. Therefore, the shifted S=O stretching frequency specifies a decline in force constant, caused by a fall in bond strength amid oxygen and sulfur due to the formation of the adduct. Therefore, the S=O stretching frequencies of both PbI_2-DMSO and MAI-PbI_2-DMSO were spotted in lower wavenumber as compared to bare

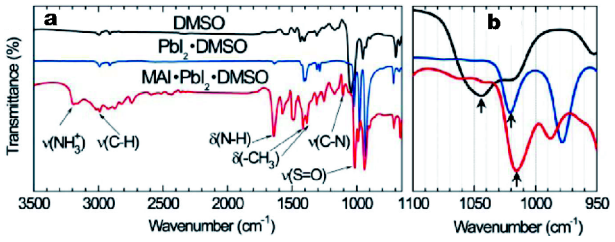

Figure 5 Fourier transform infrared spectrometer (FTIR) of (a) DMSO, PbI_2-DMSO and MAI-PbI_2-DMSO, and (b) extended fingerprint section for S=O vibrations. Reproduced from Ref. [23], Copyright 2015, American Chemical Society.

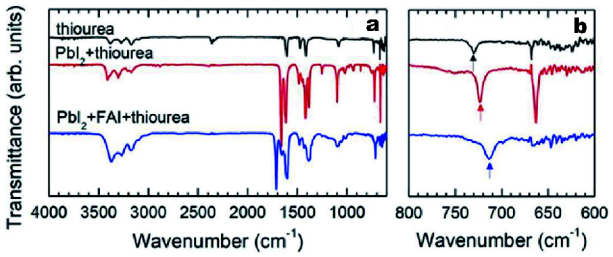

Figure 6 (a) FTIR for thiourea and its adducts, and (b) the fingerprint region for S=C stretching. Reproduced from Ref. [51], Copyright 2015, American Chemical Society.

DMSO. Since S=O stretching wavenumber of PbI_2-DMSO is higher than that of MAI-PbI_2-DMSO, it can be expected that S=O bond strength will further decrease if more Lewis acid interacts with Lewis base (DMSO) [47]. As shown in Fig. 5a, stretching peak of NH_3^+ exists in MAI-PbI_2-DMSO, showing that S=O bond strength is further reduced due to additional reaction with Lewis acid of Pb^{2+} and MA^+ ions. Hence, a stable adduct of PbI_2 and MAI is produced, as supported by Fourier transform infrared spectrometer (FTIR) study, which can result in a device with optimized morphology [23].

To further elucidate the adduct approach, Lee *et al.* [51] adopted this Lewis acid-base adduct approach on $FAPbI_3$ precursor and thiourea, a sulfur-donor as a Lewis base. For $MAPbI_3$, DMSO can be a suitable Lewis base as it possesses common $-CH_3$ functional group, while for $FAPbI_3$, the functional group of $-NH_2$ in the base was taken into consideration, since two groups of $-NH_2$ are in $FAPbI_3$. Moreover, it has been previously demonstrated that O-donors are weaker than S-donors [47]. In Fig. 6a and b, infrared spectra of FAI-PbI_2-thiourea, PbI_2-thiourea and thiourea are shown. The stretching vibration of S=C for thiourea appears at 730 cm^{-1} and indicates its change to a lower wavenumber of 724 and 714 cm^{-1} after interaction with PbI_2 only and FAI and PbI_2, correspondingly, suggestive for its adducts with both precursors [52]. This reasonable change of S=C vibration shows that thiourea robustly coordinates with FAI and PbI_2. Though the 1:1 adduct of thiourea and PbI_2 has been described earlier, the stoichiometry of the adduct of PbI_2-FAI-thiourea is not definite [47]. However, observing the clear crystal surface obtained after deposition, change of S=C stretching vibration by means of FTIR, and nominal composition of primary constituents, a 1:1:1 adduct of FAI:PbI_2:thiourea is expected to be shaped [51], leading to a good surface morphology and optimized performance with minimum hysteresis [53].

Zhang *et al.* [54] employed hexamethylphosphoramide (HMPA), a strong Lewis basic donor-solvent with a much higher electron-pair donating ability than that of DMF and DMSO, for pre-treatment of the mesoporous TiO_2 with a PbI_2 solution. By using a modified sequential deposition procedure involving a novel PbI_2-HMPA complex pre-treatment, a perovskite film with a PbI_2-rich region close to the electron transport layer was fabricated. This technique yields an average PCE as high as 19.20% with an exceptionally high FF of 0.801. This observation was ascribed to the stable adduct of HMPA with PbI_2, which successfully retarded its dissolution when depositing the perovskite layer. Due to strong Lewis basicity of HMPA, an enhanced interaction of the solvent molecules with both PbI_2 and TiO_2 was observed, which benefited the final performance of the device.

A solvent system with more than two solvents is another potential way to stretch the limits of Lewis acid-base adduct approach further. The main idea behind this technique is to wisely adjust the proportions of solvents to control the formation of IP. Wu *et al.* [55] designed a ternary mixed-solvent by adding NMP into DMF and DMSO based perovskite solution in optimized propor-

Table 1 Stretching frequency of S=O for DMSO solvent, PbI_2-DMSO and MAI-PbI_2-DMSO adducts with respective chemical structures [23]

Functional group	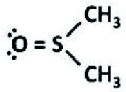	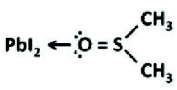	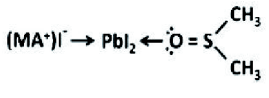
ν(S=O)	DMSO 1045 cm^{-1}	PbI_2-DMSO 1020 cm^{-1}	MAI-PbI_2-DMSO 1015 cm^{-1}

tions and fabricated a high quality mixed perovskite $Cs_{0.05}(MA_{0.17}FA_{0.83})_{0.95}Pb(I_{0.83}Br_{0.17})_3$ films. The addition of NMP causes the formation of Lewis acid-based adduct leading to slow crystallization rate and homogeneous nucleation of perovskite. Notably, the formation of the IP was controlled by tuning the NMP/DMSO ratio wisely, which resulted in the formation of enhanced perovskite films. Based on this technique, a compact, large grain, uniform film with narrower band-gap and strong absorption was prepared which showed an efficiency approaching 20%.

The action of the ternary based solvent system considerably enhanced crystals domain and produced a smooth surface with R_a value decreased to 13.9 from 25.7 as depicted in Fig. 7a and b. Fig. 7c shows that the ultraviolet-visible (UV-vis) absorption spectra of the films prepared with the ratios of 0.5:4 and 1:4 display strong absorption capacity at the wavelength over 510 nm, whereas showing less absorption capacity at the wavelength below 510 nm, which is most likely due to the defects reduction and improved crystal quality. Moreover, the perovskite films prepared by optimum ratio exhibit a red-shift in the absorption edge (Fig. 7d), indicating a better energy level and narrower band-gap, thus can grab the photons with low energy, consequent to high-efficiency device [55].

Above discussed observations advocate that adduct formation depends on not only the type of the solvent but also nature of the precursor in solution [56]. That means the acidic nature of the precursor interacting with basic solvent in solution also defines the IP induced stability and subsequent morphology. Co-solvents with more than two solvents can play a vital role in controlled nucleation by wisely adjusting the volume ratio of each, keeping solubility and physical properties of each solvent in mind. The more Lewis-acidic a precursor is, the more care should be taken while selecting solvent with high vapor pressure and low boiling point for IP formation. The high volatility of solvent will induce fast crystallization, and there will be fewer chances to form stable IP or stepwise nucleation whether it contains two or more than two co-solvents.

SOLVENT ADDITIVES

Solvent additives are one of the elements inducing enhancement of film morphology in PSCs, which are added to the solvent or solvent system. Various additives have been applied to various stoichiometry compositions. Snaith *et al.* [57] presented the use of hydro-iodic acid (HI) as a doping additive for the $FAPbI_3$ based devices. Li

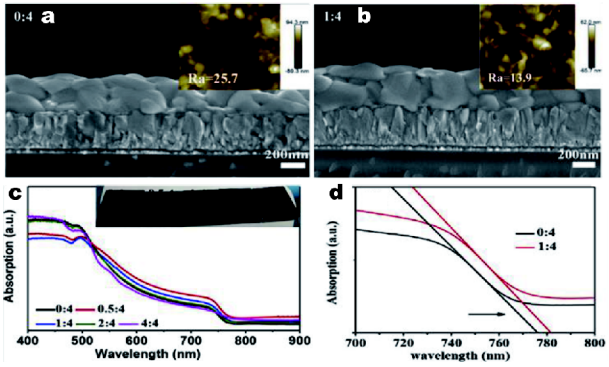

Figure 7 Cross-sectional SEM images with atomic force microscope (AFM) images of prepared films in insets (a) DMSO (without NMP, 0:4) and (b) NMP/DMSO (volume ratio of 1:4). (c) UV-vis absorption spectra of the film prepared by different NMP/DMSO volume ratios, the inset is the photos of films prepared using different volume ratios of NMP/DMSO. (d) enlargement of UV-vis absorption spectra of the films prepared by NMP/DMSO ratio with 0:4 (black) and 1:4 (red). Reproduced from Ref. [55], Copyright 2018, Elsvier.

et al. [58] added halogen acids into the PbI_2 precursor solution for the deposition of perovskite film *via* the two-step method. The impacts of hydrochloric acid (HCl) and HI on perovskite morphology, PbI_2 crystallization, stabilization and cell performance were assessed. It was shown that halogen acids boost crystal growth and homogeneous nucleation due to the modification in PbI_2 crystalline morphology. After addition of HCl or HI, the morphology of PbI_2 changes from rod-like crystals to the hexagonal plate-like crystals. The plate-like PbI_2 morphology produces complete coverage of the TiO_2 film in the planar device, which leads to complete coverage of the final perovskite film. The use of solvent additives, especially, the HCl, enhanced the device efficiency and stability. Film morphology after addition of the HI and HCl are depicted in Fig. 8. Additional additives were investigated [14,59–61].

A noticeable and exceptional solvent additive is 4-*tert*–butylpyridine (TBP), a nitrogen donor ligand, which was used in the two-step deposition after blending it into PbI_2 precursor solution [62]. When it blends into the PbI_2 precursor solution, it forms a complex of PbI_2·*x*TBP in a post DMF vaporization state, just like an adduct. The PbI_2·*x*TBP complex transforms into small pores after annealing at 70°C that can be altered using various proportions of TBP. This PbI_2 morphology enhances the diffusion of the MAI and could reduce the required time for reaction with the MAI solution. A more substantial proportion of MAI concentration gives an unceasing and smooth perovskite film without any residues of PbI_2. The device made with the TBP solvent additive exhibited vivid

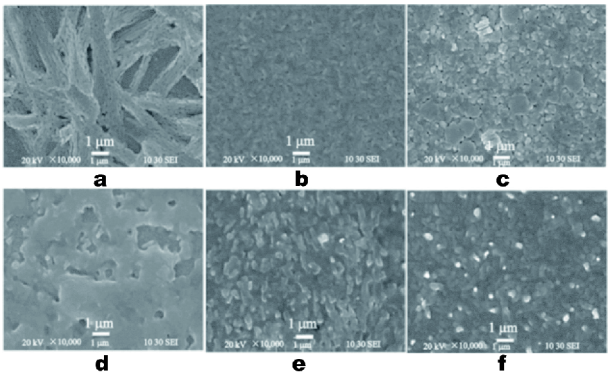

Figure 8 Surface SEM images of (a–c) pristine PbI_2, PbI_2 with HI and PbI_2 with HCl on the compact TiO_2 film. (d–f) Pristine $MAPbI_3$, $MAPbI_3$+HI, and $MAPbI_3$+HCl, respectively, after reacting with MAI. Reproduced from Ref. [58], Copyright 2015, American Chemical Society.

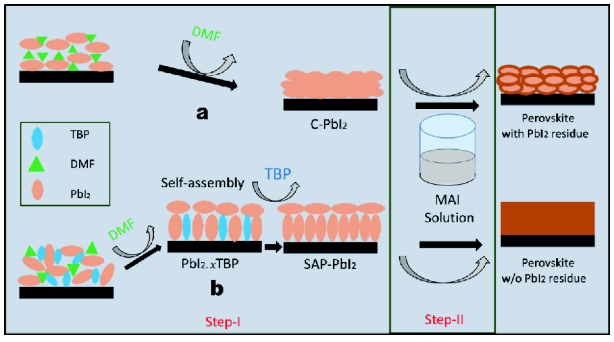

Figure 9 Schematic depiction of the PbI_2 and perovskite layers fabrication process: (a) compact PbI_2 and (b) TBP added SAP-PbI_2.

progress in performance and stability. A notable 16% efficiency was obtained for a planar structure device. The fabrication process for PbI_2 precursor with TBP as a solvent additive is schematically illustrated in Fig. 9. Shi *et al.* [63] employed the same TBP as a solvent additive in mixed halide $MAPbI_{3-x}Cl_x$ perovskite *via* one-step deposition. For a one-step route, TBP was effectively used in enhancing uniform crystallization of fine perovskite films for inverted planar structure device. The use of TBP resulted in aligned and enhanced crystallinity. Such feature imparts a positive impact on the mobility of charge carrier and subsequent performance of the PSC. Finally, the PCE of $MAPbI_{3-x}Cl_x$ based PSC exhibited a notable increase of 35% (from 11.11% to 15.01%) [63]. In another study, environmentally friendly polar aprotic solvent, 1,3-dimethyl-2-imidazolidinone (DMI) was used as a solvent additive to DMF to produce perovskite film. After addition of 10 vol% DMI in the perovskite solution, a superior film with the even surface was achieved. The average

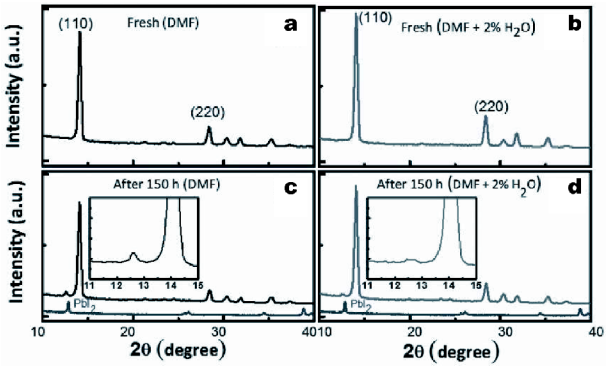

Figure 10 XRD spectra of fresh $CH_3NH_3PbI_{3-x}Cl_x$ samples based on (a) DMF, (b) DMF+water, and aged (150 h) $CH_3NH_3PbI_{3-x}Cl_x$ samples based on (c) DMF, (d) DMF+water. Reproduced from Ref. [62], Copyright 2015, Wiley-VCH GmBH&Co.

grain size grows from ~216 nm to 375 nm after annealing temperature increased from 100 to 130°C, leading to an increase in efficiency of PSCs from 10.72% to 14.54% [64]. Hence, it is a better solvent additive substitute for carcinogen HMPA and reproductive toxic NMP in producing PSCs *via* Lewis acid-base adduct approach, since it offers nontoxic working conditions [65].

Gong *et al.* [66] fabricated an efficient and resilient mixed halide perovskite film by using water as a solvent additive in the one-step deposition method. Their work obtained a device with quality crystallization and resistance against humidity. Water molecules were added into DMF solution to tune the growth of crystals as water has a lower boiling point and higher vapor pressure. After the addition of 2% deionized water, good film coverage with improved grain size was observed. It was stated that $CH_3NH_3PbI_{3-x}Cl_x{\cdot}nH_2O$ hydrated perovskites were assumed to be generated during the annealing process, which can be resilient to the corrosion by humidity to some degree. As shown in Fig. 10. compared with the fresh samples, a peak at 12.65°, was observed in aged $CH_3NH_3PbI_{3-x}Cl_x$ samples with and without water additive. Meanwhile, the strengths of the (110) and (220) peaks were visibly weakened compared with the fresh ones. The presence of (001) peak at 12.65° supports that $CH_3NH_3PbI_{3-x}Cl_x$ films experienced decomposition due to continued exposure in ambient, which results in the generation of PbI_2. Notably, the intensity of (001) peak at 12.65° in water additive based samples is lower than that in without water-based samples. It shows that water additive based perovskite can resist the decomposition in humid circumstances to some degree, which leads to enhanced cell stability.

Although water is not a strong solvent to dissolve the

perovskite precursor, its physical properties made it useful in above-discussed finding. Acetonitrile (ACN) is another weak molecule used for perovskite film enhancement. Liang *et al.* [67] used ACN as a solvent additive along with DMF and DMSO in a two-step method and found that certain amount of ACN in solution can enhance the film quality and subsequent performance. The different molar ratio of ACN and DMSO were added in DMF to study the effect. It was observed that ACN based samples show better morphological features with large grain dimensions than DMSO based samples. The enhanced grain dimensions imply that the addition of ACN not only preserve the film morphology but also essentially mediate the dynamics of crystallization. This finding proposes that the solvent additives with different coordination ability can be vital to the film crystallization process.

Solvent additives can serve as the active agents for altering the perovskite layer as per required structural growth with feasible device characteristics in respective deposition route, which can be one-step or two-step method. Some additive can trigger the fast crystallization, while some can delay the nucleation process, depending on their nature. Additives with different or weak coordination strength can still play a key role in desired results if used in suitable deposition route combined with primary solvents. In one word, these solvents work as a modifier to give a finish to the film for optimized performances.

SOLVENT COORDINATION PROPERTIES

Crystallization routes for perovskite and the efficiency of PSCs containing the subsequent active layers have been influenced by the existence of solution based complex intermediates [68–72]. It is generally believed that the choice of solvent tells the formation of these complex intermediates [71,73]. However, which mechanism the coordination of solvent precursor affects crystallization process, what properties of the solvent states these interactions and how it influences the intermediates formation are not entirely understood. So far, Mayer bond unsaturation, Hansen's solubility parameters, dielectric constant and donor number (D_N) [71,74–77] have been used to define the interactions among solvent and precursors in perovskite solution. The dielectric constant of the aprotic solvent is believed to relate with its "coordinating strength" with the precursors particularly lead halides [71], which affects the intermediates formation of iodoplumbate (PbI_n^{2-n}, n = 2−6) as well as lead−solvent complexes [71] in solutions containing methylammonium iodide and lead halide. The presence of such complexes consequently defines the film morphology and defect density of the whole perovskite films [69]. It is determined that strong coordinating solvents will mainly produce less number of iodide ions complexes and weak coordinating solvents produce a large number of PbI_6^- complexes. It also suggests that all of these plumbate ions might serve as a source of structural defects defining electronic characteristics of the perovskite films [71]. While on the other side, Saidaminov *et al.* [74] revealed that single crystals of $MAPbI_3$ can be grown from GBL instead of DMF [78] and then differences in polarity were proved as a reason of various coordinating abilities of the solvents for such behaviour. Furthermore, Hansen's solubility parameters, have been proposed as a preliminary idea to choose solvents [75,77].

Gardner *et al.* [75] adopted the Hansen solubility parameter model to set a rule for a possible combination blend of non-hazardous solvents for the fabrication of perovskite film and presented a starting point for non-hazardous solvent systems for one-step deposition of perovskite (with spectator ion) films processed by alcohol, acid and solvent blends. By using GBL/ethanol/acetic acid (60/20/20 vol%), 15.1% of PCE was attained. After maximum power point tracking for 5 min and exposed to continuous illumination, the maximum power point of PCE was maintained at 13.5%, comparable to that of DMF-based PSCs [75]. However, Hansen's solubility parameters fail for an explanation of molecular complexion and ionic interactions [75,77].

Hamill *et al.* [77] elucidated the strength of processing solvent using Lewis basicity, equated by Gutmann's donor number, D_N, on perovskite formation. They advocated that D_N is a more robust indicator for the ability of solvents to dissolve perovskite precursor instead of dielectric constant since the D_N defines the potency of interactions amongst Lewis basic solvent and marginal soft Lewis acidic Pb^{2+} center of iodoplumbate complex in the precursor solution. Solvents with high D_N number contest with I^- for coordination site about Pb^{2+} and subsequently reduce the iodoplumbates formation; these Lewis solvents form a steady perovskite solution for thin-film fabrication. Solvents with low-D_N coordinate weakly with Pb^{2+} and therefore support the formation of iodoplumbate and consequent single crystal evolution. This notion assists the careful choice of solvent additives or processing solvents tailored for the preferred use [77]. Fig. 11a shows a weaker relation among the dielectric constants of basic solvents and the solvent's ability to produce stable perovskite solution. In broad terms, persistent with whatever

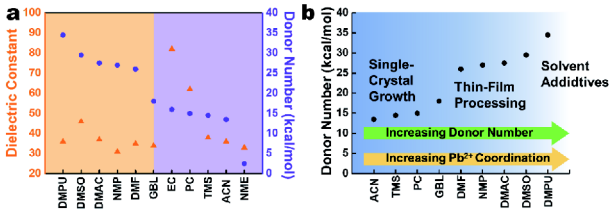

Figure 11 (a) Gutmann's donor number (D_N) and dielectric constant of solvents used for PSCs. The solvents that can form a stable precursor solution at total MAI and PbI_2 concentrations surpassing 1 mol L^{-1} are shown in the unshaded area on the left. The solvents cannot form the stable solution. Instead, crystals evolve naturally and precipitate from solution shown in a shaded area on the right. (b) Elucidating the relation between D_N and Pb^{2+} coordination.

has been stated in the previous research [23,51,75], solvents with dielectric constants greater than 30 seem to solubilize the perovskite precursors. However, facts shed light on much exclusion to this statement. Such as ACN and tetramethylsulfone (TMS) with dielectric constants more than 30, cannot form a stable precursor solution; instead, the precursors readily crystallize to $MAPbI_3$. Propylene carbonate (PC) and ethylene carbonate (EC) have higher dielectric constants compared to the other tested solvents; these two solvents do not form the steady precursor solutions. Lastly, nitro-methane (NME), with the dielectric constant of 35.9, does not solubilize the precursors completely.

It is shown that the D_N displays a strong relation with the potency of the solvent to dissolve the perovskite precursor. Solvents with the D_N greater than 18 kcal mol^{-1} are good to solubilize the precursors, while solvents with the D_N less than 18 kcal mol^{-1} supports crystallization of the perovskite precursors from 1 mol L^{-1} solution. Indeed, precursor solutions in solvents having the D_N greater than 18 kcal mol^{-1} are steady even after heated near to the solvent's boiling point temperatures. It can be concluded that the D_N is a reliable indicator of solubility than dielectric constant, showing that Lewis acid-base coordination amongst the precursor and solvent, not electrostatics, rules the dissolution process. Since the Pb^{2+} center of the acidic lead salt shows an affinity for Lewis basic ligand group, which may be solvent molecules, iodide anions or their combination [71,73]. The strength of the lead salt to be solubilized improves when its affinity for the Lewis ligands improves [77].

This base formed the framework with which solvents having high D_N can be selected as a solvent or additives to modify the morphology of the thin film and better flexibility in the post-deposition process. It highlights the sort of physical indicators that can promote the solvent–precursor interactions in solutions and shows that the sensible choice of solvents or additives is essential to alter solid-state structural growth in PSCs.

SUMMARY

This review commented the dynamics of current and potential practices of solvent engineering to make an enhanced and vibrant perovskite device. Solvents were discussed for one-step and two-step deposition method regarding primary solvent and co-solvent (solvent system) with respective outcomes. Solvents were differentiated *via* coordinating with the precursor. It is evident that DMF and DMSO are stronger to dissolve precursor compared with others, which can lead to better morphology with fewer trap states. Lewis acid-base adduct approach for controlled nucleation and retarded crystallization were explained to make it easy to understand the role of stable intermediate complex amongst precursor and solvent (or solvent system) for the enhanced morphology and better performance. Strong solvents with a high boiling point like DMSO and thiourea are concluded as a suitable option for stable adduct with the precursor, which in turn retards nucleation rate and makes the uniform growth of grains possible. Later, the influence of different solvent additive with the resulting desired structure and optimized performance was elaborated. In the end, a framework for judicious selection of solvent by varying coordination properties was sketched. After discussing different coordination properties, Gutmann's D_N was aligned with solvent's strength of coordination with the precursor to making a sensible choice of solvent for desired perovskite solution.

Received 6 June 2018; accepted 9 August 2018; published online 18 September 2018

1 Cheng Z, Lin J. Layered organic–inorganic hybrid perovskites: structure, optical properties, film preparation, patterning and templating engineering. CrystEngComm, 2010, 12: 2646
2 Stranks SD, Eperon GE, Grancini G, *et al.* Electron-hole diffusion lengths exceeding 1 micrometer in an organometal trihalide perovskite absorber. Science, 2013, 342: 341–344
3 Ren YK, Ding XH, Wu YH, *et al.* Temperature-assisted rapid nucleation: a facile method to optimize the film morphology for perovskite solar cells. J Mater Chem A, 2017, 5: 20327–20333
4 Liu C, Yang Y, Ding Y, *et al.* High-efficiency and UV-stable planar perovskite solar cells using a low-temperature, solution-processed electron-transport layer. ChemSusChem, 2018, 11: 1232–1237
5 Im JH, Lee CR, Lee JW, *et al.* 6.5% efficient perovskite quantum-dot-sensitized solar cell. Nanoscale, 2011, 3: 4088–4093
6 Yang WS, Park BW, Jung EH, *et al.* Iodide management in formamidinium-lead-halide–based perovskite layers for efficient solar cells. Science, 2017, 356: 1376–1379
7 Green MA, Emery K, Hishikawa Y, *et al.* Solar cell efficiency tables

(version 46). Prog Photovolt-Res Appl, 2015, 23: 805–812
8 Xing G, Mathews N, Sun S, *et al.* Long-range balanced electron- and hole-transport lengths in organic-inorganic $CH_3NH_3PbI_3$. Science, 2013, 342: 344–347
9 Shi D, Adinolfi V, Comin R, *et al.* Low trap-state density and long carrier diffusion in organolead trihalide perovskite single crystals. Science, 2015, 347: 519–522
10 Liu M, Johnston MB, Snaith HJ. Efficient planar heterojunction perovskite solar cells by vapour deposition. Nature, 2013, 501: 395–398
11 Burschka J, Pellet N, Moon SJ, *et al.* Sequential deposition as a route to high-performance perovskite-sensitized solar cells. Nature, 2013, 499: 316–319
12 Chen Q, Zhou H, Hong Z, *et al.* Planar heterojunction perovskite solar cells *via* vapor-assisted solution process. J Am Chem Soc, 2014, 136: 622–625
13 Xiao M, Huang F, Huang W, *et al.* A fast deposition-crystallization procedure for highly efficient lead iodide perovskite thin-film solar cells. Angew Chem Int Ed, 2014, 53: 9898–9903
14 Liang PW, Liao CY, Chueh CC, *et al.* Additive enhanced crystallization of solution-processed perovskite for highly efficient planar-heterojunction solar cells. Adv Mater, 2014, 26: 3748–3754
15 Jeon NJ, Noh JH, Kim YC, *et al.* Solvent engineering for high-performance inorganic–organic hybrid perovskite solar cells. Nat Mater, 2014, 13: 897–903
16 Yakunin S, Sytnyk M, Kriegner D, *et al.* Detection of X-ray photons by solution-processed lead halide perovskites. Nat Photonics, 2015, 9: 444–449
17 Luo J, Im JH, Mayer MT, *et al.* Water photolysis at 12.3% efficiency *via* perovskite photovoltaics and earth-abundant catalysts. Science, 2014, 345: 1593–1596
18 Dong Q, Fang Y, Shao Y, *et al.* Electron-hole diffusion lengths >175 μm in solution-grown $CH_3NH_3PbI_3$ single crystals. Science, 2015, 347: 967–970
19 de Quilettes DW, Vorpahl SM, Stranks SD, *et al.* Impact of microstructure on local carrier lifetime in perovskite solar cells. Science, 2015, 348: 683–686
20 Stranks SD, Burlakov VM, Leijtens T, *et al.* Recombination kinetics in organic-inorganic perovskites: excitons, free charge, and subgap states. Phys Rev Appl, 2014, 2: 034007
21 Mehmood U, Al-Ahmed A, Afzaal M, *et al.* Recent progress and remaining challenges in organometallic halides based perovskite solar cells. Renew Sust Energ Rev, 2017, 78: 1–14
22 Yang WS, Noh JH, Jeon NJ, *et al.* High-performance photovoltaic perovskite layers fabricated through intramolecular exchange. Science, 2015, 348: 1234–1237
23 Ahn N, Son DY, Jang IH, *et al.* Highly reproducible perovskite solar cells with average efficiency of 18.3% and best efficiency of 19.7% fabricated *via* lewis base adduct of lead(II) iodide. J Am Chem Soc, 2015, 137: 8696–8699
24 Kim HB, Choi H, Jeong J, *et al.* Mixed solvents for the optimization of morphology in solution-processed, inverted-type perovskite/fullerene hybrid solar cells. Nanoscale, 2014, 6: 6679–6683
25 Lian J, Wang Q, Yuan Y, *et al.* Organic solvent vapor sensitive methylammonium lead trihalide film formation for efficient hybrid perovskite solar cells. J Mater Chem A, 2015, 3: 9146–9151
26 Cai B, Zhang WH, Qiu J. Solvent engineering of spin-coating solutions for planar-structured high-efficiency perovskite solar cells. Chin J Catal, 2015, 36: 1183–1190
27 Song TB, Chen Q, Zhou H, *et al.* Perovskite solar cells: film formation and properties. J Mater Chem A, 2015, 3: 9032–9050
28 Wu Y, Islam A, Yang X, *et al.* Retarding the crystallization of PbI_2 for highly reproducible planar-structured perovskite solar cells *via* sequential deposition. Energy Environ Sci, 2014, 7: 2934–2938
29 Chen J, Xiong Y, Rong Y, *et al.* Solvent effect on the hole-conductor-free fully printable perovskite solar cells. Nano Energy, 2016, 27: 130–137
30 Lin SQ, Li W, Sun, HC, et al. Effects of different solvents on the planar hetero-junction perovskite solar cells. ICETA, 2015, 22: 05002
31 Seo YH, Kim EC, Cho SP, *et al.* High-performance planar perovskite solar cells: Influence of solvent upon performance. Appl Mater Today, 2017, 9: 598–604
32 Guo X, McCleese C, Kolodziej C, *et al.* Identification and characterization of the intermediate phase in hybrid organic–inorganic $MAPbI_3$ perovskite. Dalton Trans, 2016, 45: 3806–3813
33 Nie W, Tsai H, Asadpour R, *et al.* High-efficiency solution-processed perovskite solar cells with millimeter-scale grains. Science, 2015, 347: 522–525
34 Aldibaja FK, Badia L, Mas-Marzá E, *et al.* Effect of different lead precursors on perovskite solar cell performance and stability. J Mater Chem A, 2015, 3: 9194–9200
35 Xie FX, Zhang D, Su H, *et al.* Vacuum-assisted thermal annealing of $CH_3NH_3PbI_3$ for highly stable and efficient perovskite solar cells. ACS Nano, 2015, 9: 639–646
36 Fang X, Wu Y, Lu Y, *et al.* Annealing-free perovskite films based on solvent engineering for efficient solar cells. J Mater Chem C, 2017, 5: 842–847
37 Dubey A, Kantack N, Adhikari N, *et al.* Room temperature, air crystallized perovskite film for high performance solar cells. J Mater Chem A, 2016, 4: 10231–10240
38 Zuo L, Dong S, De Marco N, *et al.* Morphology evolution of high efficiency perovskite solar cells *via* vapor induced intermediate phases. J Am Chem Soc, 2016, 138: 15710–15716
39 Rong Y, Tang Z, Zhao Y, *et al.* Solvent engineering towards controlled grain growth in perovskite planar heterojunction solar cells. Nanoscale, 2015, 7: 10595–10599
40 Wakamiya A, Endo M, Sasamori T, *et al.* Reproducible fabrication of efficient perovskite-based solar cells: X-ray crystallographic studies on the formation of $CH_3NH_3PbI_3$ layers. Chem Lett, 2014, 43: 711–713
41 Li W, Fan J, Li J, *et al.* Controllable grain morphology of perovskite absorber film by molecular self-assembly toward efficient solar cell exceeding 17%. J Am Chem Soc, 2015, 137: 10399–10405
42 Miyamae H, Numahata Y, Nagata M. The crystal structure of lead (II) iodide-dimethylsulphoxide(1/2), $PbI_2(DMSO)_2$. Chem Lett, 1980, 9: 663–664
43 Dualeh A, Tétreault N, Moehl T, *et al.* Effect of annealing temperature on film morphology of organic-inorganic hybrid perovskite solid-state solar cells. Adv Funct Mater, 2014, 24: 3250–3258
44 Ren Y, Duan B, Xu Y, *et al.* New insight into solvent engineering technology from evolution of intermediates *via* one-step spin-coating approach. Sci China Mater, 2017, 60: 392–398
45 Krautscheid H, Vielsack F. Discrete and polymeric iodoplumbates with Pb_3I_{10} building blocks: $[Pb_3I_{10}]^{4-}$, $[Pb_7I_{22}]^{8-}$, $[Pb_{10}I_{28}]^{8-}$, $^1_\infty[Pb_3I_{10}]^{4-}$ and $^2_\infty[Pb_7I_{18}]^{4-}$. Dalton Trans, 1999, 16: 2731–2735
46 Krautscheid H, Vielsack F. $[BuN(CH_2CH_2)_3NBu]_3[Pb_5I_{16}]\cdot 4DMF$–ein Iodoplumbat mit Nahe zu D_{5h}-symmetrischem Anion. Z Anorg Allg Chem, 2000, 626: 3–5

47 Wharf I, Gramstad T, Makhija R, *et al.* Synthesis and vibrational spectra of some lead(II) halide adducts with O-, S-, and N-donor atom ligands. Can J Chem, 1976, 54: 3430–3438
48 Ren YK, Liu SD, Duan B, *et al.* Controllable intermediates by molecular self-assembly for optimizing the fabrication of large-grain perovskite films *via* one-step spin-coating. J Alloys Compd, 2017, 705: 205–210
49 Pavia DL, Lampman GM, Kriz GS, *et al.* Introduction to Spectroscopy (4th Edition). Belmont: Cengage Learning, 2009
50 Colthup NB, Daly LH, Wiberley SE. Introduction to Infrared and Raman Spectroscopy (Second Edition). New York: Academic Press, 1975
51 Lee JW, Kim HS, Park NG. Lewis acid–base adduct approach for high efficiency perovskite solar cells. Acc Chem Res, 2016, 49: 311–319
52 Madhurambal G, Mariappan M, Mojumdar SC. TG–DTA, UV and FTIR spectroscopic studies of urea–thiourea mixed crystal. J Therm Anal Calorim, 2010, 100: 853–856
53 Seo YH, Kim EC, Cho SP, *et al.* Hysteresis data of planar perovskite solar cells fabricated with different solvents. Data Brief, 2018, 16: 418–422
54 Zhang Y, Gao P, Oveisi E, *et al.* PbI_2–HMPA complex pretreatment for highly reproducible and efficient $CH_3NH_3PbI_3$ perovskite solar cells. J Am Chem Soc, 2016, 138: 14380–14387
55 Wu T, Wu J, Tu Y, *et al.* Solvent engineering for high-quality perovskite solar cell with an efficiency approaching 20%. J Power Sources, 2017, 365: 1–6
56 Hao F, Stoumpos CC, Guo P, *et al.* Solvent-mediated crystallization of $CH_3NH_3SnI_3$ films for heterojunction depleted perovskite solar cells. J Am Chem Soc, 2015, 137: 11445–11452
57 Eperon GE, Stranks SD, Menelaou C, *et al.* Formamidinium lead trihalide: a broadly tunable perovskite for efficient planar heterojunction solar cells. Energy Environ Sci, 2014, 7: 982
58 Yang L, Wang J, Leung WWF. Lead iodide thin film crystallization control for high-performance and stable solution-processed perovskite solar cells. ACS Appl Mater Interfaces, 2015, 7: 14614–14619
59 Carnie MJ, Charbonneau C, Davies ML, *et al.* A one-step low temperature processing route for organolead halide perovskite solar cells. Chem Commun, 2013, 49: 7893
60 Zhao Y, Zhu K. CH_3NH_3Cl-assisted one-step solution growth of $CH_3NH_3PbI_3$: structure, charge-carrier dynamics, and photovoltaic properties of perovskite solar cells. J Phys Chem C, 2014, 118: 9412–9418
61 Chang CY, Chu CY, Huang YC, *et al.* Tuning perovskite morphology by polymer additive for high efficiency solar cell. ACS Appl Mater Interfaces, 2015, 7: 4955–4961
62 Zhang H, Mao J, He H, *et al.* A smooth $CH_3NH_3PbI_3$ film *via* a new approach for forming the PbI_2 nanostructure together with strategically high CH_3NH_3I concentration for high efficient planar-heterojunction solar cells. Adv Energy Mater, 2015, 5: 1501354
63 Shi Y, Wang X, Zhang H, *et al.* Effects of 4-*tert*-butylpyridine on perovskite formation and performance of solution-processed perovskite solar cells. J Mater Chem A, 2015, 3: 22191–22198
64 Zhi L, Li Y, Cao X, *et al.* Perovskite solar cells fabricated by using an environmental friendly aprotic polar additive of 1,3-dimethyl-2-imidazolidinone. Nanoscale Res Lett, 2017, 12: 632
65 Lo CC, Chao PM. Replacement of carcinogenic solvent HMPA by DMI in insect sex pheromone synthesis. J Chem Ecol, 1990, 16: 3245–3253
66 Gong X, Li M, Shi XB, *et al.* Controllable perovskite crystallization by water additive for high-performance solar cells. Adv Funct Mater, 2015, 25: 6671–6678
67 Li L, Chen Y, Liu Z, *et al.* The additive coordination effect on hybrids perovskite crystallization and high-performance solar cell. Adv Mater, 2016, 28: 9862–9868
68 Stamplecoskie KG, Manser JS, Kamat PV. Dual nature of the excited state in organic–inorganic lead halide perovskites. Energy Environ Sci, 2015, 8: 208–215
69 Stewart RJ, Grieco C, Larsen AV, *et al.* Molecular origins of defects in organohalide perovskites and their influence on charge carrier dynamics. J Phys Chem C, 2016, 120: 12392–12402
70 Yoon SJ, Stamplecoskie KG, Kamat PV. How lead halide complex chemistry dictates the composition of mixed halide perovskites. J Phys Chem Lett, 2016, 7: 1368–1373
71 Rahimnejad S, Kovalenko A, Forés SM, *et al.* Coordination chemistry dictates the structural defects in lead halide perovskites. ChemPhysChem, 2016, 17: 2795–2798
72 Sharenko A, Mackeen C, Jewell L, *et al.* Evolution of iodoplumbate complexes in methylammonium lead iodide perovskite precursor solutions. Chem Mater, 2017, 29: 1315–1320
73 Manser JS, Saidaminov MI, Christians JA, *et al.* Making and breaking of lead halide perovskites. Acc Chem Res, 2016, 49: 330–338
74 Saidaminov MI, Abdelhady AL, Maculan G, *et al.* Retrograde solubility of formamidinium and methylammonium lead halide perovskites enabling rapid single crystal growth. Chem Commun, 2015, 51: 17658–17661
75 Gardner KL, Tait JG, Merckx T, *et al.* Nonhazardous solvent systems for processing perovskite photovoltaics. Adv Energy Mater, 2016, 6: 1600386
76 Stevenson J, Sorenson B, Subramaniam VH, *et al.* Mayer bond order as a metric of complexation effectiveness in lead halide perovskite solutions. Chem Mater, 2017, 29: 2435–2444
77 Hamill Jr. JC, Schwartz J, Loo YL. Influence of solvent coordination on hybrid organic–inorganic perovskite formation. ACS Energy Lett, 2018, 3: 92–97
78 Saidaminov MI, Abdelhady AL, Murali B, *et al.* High-quality bulk hybrid perovskite single crystals within minutes by inverse temperature crystallization. Nat Commun, 2015, 6: 7586

Acknowledgements This work was supported by the National Key Research and Development Program of China (2016YFA0202400), the 111 project (B16016), and the National Natural Science Foundation of China (51572080, 51702096, and U1705256).

Author contributions Arain Z performed the main analysis and wrote this manuscript. Ding Y directly guided and conducted this research including the design, modifying and polishing work related to this manuscript. Dai S supervised the project and carefully reviewed this manuscript. Liu C, Yang Y, Mateen M, Ren Y, Liu X provided help in the collection of data. Ali Z and Kumar M worked as a supporting advisor to improve the quality of work. All authors contributed to the general discussion about this work.

Conflict of interest The authors declare no conflict of interest.

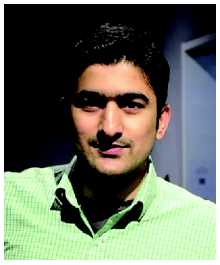

Zulqarnain Arain obtained his BSc degree from QUEST University, Pakistan in 2014. He is a Master student of the North China Electric Power University under the supervision of Prof. Yong Ding and Prof. Songyuan Dai. He is also a faculty member of Energy System Engineering Dept. SIBA University, Pakistan and currently on study Leave. His research interest mainly focuses on perovskite solar cells.

Yong Ding is a lecturer in Beijing Key Lab of Novel Thin Film Solar Cells, North China Electric Power University. He received his PhD degree in physical chemistry from Hefei Institutes of Physical Science, Chinese Academy of Sciences in 2011. His research interest is novel-type solar cells, including dye-sensitized solar cells and perovskite solar cells.

Songyuan Dai is a professor and Dean of the School of Renewable Energy, North China Electric Power University. He obtained his BSc degree in physics from Anhui Normal University in 1987, and MSc and PhD degrees in plasma physics from the Institute of Plasma Physics, Chinese Academy of Sciences in 1991 and 2001, respectively. His research interest mainly focuses on the next-generation solar cells including dye-sensitized solar cells, quantum dot solar cells, perovskite solar cells, etc.

钙钛矿太阳电池溶剂工程的动力学阐述

Zulqarnain Arain[1,3], 刘成[1], 杨熠[1], M. Mateen[1], 任英科[1], 丁勇[1*], 刘雪朋[1], Zulfiqar Ali[2], Manoj Kumar[3], 戴松元[1*]

摘要 光伏领域的研究者们在不断探索可以用于高效太阳能转换的新材料. 研究每种新型光伏材料的主要目的是通过简单的制造工艺和较低的生产成本来实现更高的能量产出. 新兴的钙钛矿材料也在竞争行列之中. 通过不同的化学计量调控和工艺改进, 钙钛矿太阳电池在过去的几年中实现了最高的光电转换效率, 这一技术已经成为未来能量转换材料的有力候选者. 到目前为止, 许多研究表明活性层的薄膜质量在很大程度上决定了钙钛矿太阳电池的光电性能. 当前和潜在的用于制备良好活性层形貌的溶剂工程技术大体上是使用主要溶剂、共溶剂(路易斯酸-碱加合方法)和溶剂添加剂来实现. 在这篇综述中, 我们详细讨论了多种已报道的溶剂工程动力学对钙钛矿太阳电池活性层形态特征的影响. 目的是通过不同的结晶过程得到一个关于溶剂工程如何诱导钙钛矿太阳电池活性层形貌的清晰的认知. 最后, 我们基于不同溶剂的配位性质绘制了一个基本框架, 便于筛选可用来制备钙钛矿前驱体的有效溶剂, 以获得性能更好和可行性更高的光伏器件.

